ISSN 1674-1056
http://cpb.iphy.ac.cn
http://iopscience.iop.org/cpb
中国物理 B
Chinese Physics
中国物理 Chinese Physics B

Analysis of highly efficient perovskite solar cells with inorganic hole transport material

I Kabir, S A Mahmood
Citation: Chin. Phys. B . 2019, 28(12): 128801 . **doi:** 10.1088/1674-1056/ab520f
Journal homepage: http://cpb.iphy.ac.cn; http://iopscience.iop.org/cpb

What follows is a list of articles you may be interested in

Effect of carrier mobility on performance of perovskite solar cells

Yi-Fan Gu(顾一帆), Hui-Jing Du(杜会静), Nan-Nan Li(李楠楠), Lei Yang(杨蕾), Chun-Yu Zhou(周春宇)
Chin. Phys. B . 2019, 28(4): 048802 . **doi:** 10.1088/1674-1056/28/4/048802

Insight into band alignment of Zn(O,S)/CZTSe solar cell by simulation

Zhen-Wu Jiang(姜振武), Shou-Shuai Gao(高守帅), Si-Yu Wang(王思宇), Dong-Xiao Wang(王东潇), Peng Gao(高鹏), Qiang Sun(孙强), Zhi-Qiang Zhou(周志强), Wei Liu(刘玮), Yun Sun(孙云), Yi Zhang(张毅)
Chin. Phys. B . 2019, 28(4): 048801 . **doi:** 10.1088/1674-1056/28/4/048801

Theoretical study on the kesterite solar cells based on $Cu_2ZnSn(S,Se)_4$ and related photovoltaic semiconductors

Dingrong Liu(刘定荣), Dan Han(韩丹), Menglin Huang(黄梦麟), Xian Zhang(张弦), Tao Zhang(张涛), Chenmin Dai(戴称民), Shiyou Chen(陈时友)
Chin. Phys. B . 2018, 27(1): 018806 . **doi:** 10.1088/1674-1056/27/1/018806

Promise of commercialization: Carbon materials for low-cost perovskite solar cells

Yu Cai(蔡宇), Lusheng Liang(梁禄生), Peng Gao(高鹏)
Chin. Phys. B . 2018, 27(1): 018805 . **doi:** 10.1088/1674-1056/27/1/018805

420 nm thick $CH_3NH_3PbI_{3-x}Br_x$ capping layers for efficient TiO_2 nanorod array perovskite solar cells

Long Li(李龙), Cheng-Wu Shi(史成武), Xin-Lian Deng(邓新莲), Yan-Qing Wang(王艳青), Guan-Nan Xiao(肖冠南), Ling-Ling Ni(倪玲玲)
Chin. Phys. B . 2018, 27(1): 018804 . **doi:** 10.1088/1674-1056/27/1/018804

Analysis of highly efficient perovskite solar cells with inorganic hole transport material

I Kabir and S A Mahmood†

Department of Electrical and Electronics Engineering, Bangladesh University of Engineering and Technology, Dhaka, Bangladesh

(Received 8 July 2019; revised manuscript received 29 September 2019; published online 29 November 2019)

Organo-halide perovskites in planar heterojunction architecture have shown considerable promise as efficient light harvesters in solar cells. We carry out a numerical modeling of a planar lead based perovskite solar cell (PSC) with Cu_2ZnSnS_4 (CZTS) as the hole transporting material (HTM) using the one-dimensional solar cell capacitance simulator (SCAPS-1D). The effects of numerous parameters such as defect density, thickness, and doping density of the absorber layer on the device performance are investigated. The doping densities and electron affinities of the electron transporting material (ETM) and the HTM are also varied to optimize the PSC performance. It has been observed that a thinner absorber layer of $\sim$220 nm with a defect density of 10^{14} cm^{-3} compared to the reference structure improves the device performance. When doping density of the absorber layer increases beyond 2×10^{16} cm^{-3}, the power conversion efficiency (PCE) reduces due to enhanced recombination rate. The defect density at the absorber/ETM interface reduces the PCE as well. Considering a series resistance of 5 $\Omega\cdot$cm^2 and all the optimum parameters of absorber, ETM and HTM layers simultaneously, the overall PCE of the device increases significantly. In comparison with the reference structure, the PCE of the optimized device has been increased from 12.76% to 22.7%, and hence the optimized CZTS based PSC is highly efficient.

Keywords: $CH_3NH_3PbI_3$, Cu_2ZnSnS_4 (CZTS), SCAPS-1D, absorption coefficient

PACS: 88.40.H–, 88.40.hj, 88.40.fc **DOI:** 10.1088/1674-1056/ab520f

1. Introduction

The rate of energy consumption increases to cope with economic development. However the source of nonrenewable energy decreases gradually. Among other renewable energy sources, solar cells have drawn a great deal of attention from researchers. Over the past decade, many studies have been carried out on organo-halide perovskite solar cells (PSCs).[1–4] In comparison with traditional solar cells, they have simpler processing techniques, higher power conversion efficiency (PCE), and lower cost.[5] In 2009, Miyasaka *et al.* first introduced the PSCs using $MAPbI_3$ ($MA=CH_3NH_3$) and $MAPbBr_3$ as light harvesters although their PCEs are low (3%–4%).[6] Recently, the PCEs of lead based PSCs have reached $\sim$22.1%.[1,7] The PCEs have reached above 25% when PSC is used in silicon based tandem solar cells.[8] The absorption coefficient of $MAPbX_3$ is very high (10^3–10^4 cm^{-1}) along with high charge carrier mobility (2–66 cm$^2\cdot$V$^{-1}\cdot$s^{-1}).[7] The tunable band gap (1.55–2.50 eV) property of this material can be utilized to make colorful solar designs.[9] In addition, $MAPbX_3$ based thin films have charge carrier life time of $\sim$270 ns and carrier diffusion length of 100–1900 nm.[7]

The planar PSC structure, where a thin perovskite layer is sandwiched between layers of a hole transporting material (HTM) and an electron-transporting material (ETM), is preferred due to simple fabrication technique.[10] According to the order of preparation, the planar PSC structure can be either n–i–p or p–i–n. Organic compounds, such as spiro-MeOTAD, PEDOT:PSS, PTAA and P3HT are the commonly used HTMs in the case of high-efficient PSCs.[2,11–13] However, most of the organic based HTMs are unstable and costly. The reduction in PCE of spiro-MeOTAD based PSC is more than 50% after 15 days under moisture and heat.[14] The complex and time consuming synthetic process make the spiro-MeOTAD based PSCs costly as well.[2] PEDOT:PSS is chemically unstable due to its acidic and hygroscopic nature.[15] The contraction of PEDOT conductive grains leads to the thermal instability of PEDOT:PSS films.[15] The PCE of PEDOT:PSS based PSC reduces by 40% within 10 days.[16] The highest PCE achieved by PTAA based PSC is 21.2% and the PCE degradation is $\sim$5% in 20 days.[11,17] The PCE of pristine P3HT based PSC is only 14.3% and degraded by 20% within 29 days.[18]

Inorganic HTMs are preferable as they are cheaper, more stable, and simple to synthesize. Recently, Cu based HTMs such as CuI, CuSCN, Cu_2O, CuInGaSSe, and Cu_2ZnSnS_4 (CZTS) draw attention of researchers.[19–23] The reported PCE of CuI based PSC is 17.6% and the PCE decreases by 8% within 90 days.[22] Although its stability is comparable to PTAA based PSC, the PCE is lower than the organic counterpart. Its mesoporous structure increases the process complexity and hence industrially less preferable.[24] The PCE of CuSCN based inverted planar PSC is 15.6% and degraded by 20% within 2 days.[19] A PCE of 13.35% is achieved by Cu_2O based inverted planar PSC and sustained above 90% of initial value for 70 days.[20] Another mesostructured PSC with CuIn-

†Corresponding author. E-mail: asifmahmood@eee.buet.ac.bd

© 2019 Chinese Physical Society and IOP Publishing Ltd

GaSSe as HTM achieves a PCE of 9.15% and sustained 90% of initial value for 5 days. Kesterite materials, e.g., CZTS, are an efficient light harvester for thin film solar cells due to their high absorption coefficient ($\sim 10^4$ cm^{-1}), optimal band gap (1.4–1.5 eV) for solar energy conversion, high hole mobility (6–35 cm^2·V^{-1}·s^{-1}), and earth abundant constituents.[25] However, the highest PCE of CZTSSe based thin film solar cell is 12.6%.[21] Wu *et al.* have shown that Cu_2ZnSnS_4 (CZTS) can be used as a nontoxic and low cost HTM in planar lead based PSC.[25] It increases the light absorbance of the device and hence increases the short circuit current density of the PSC. Surface recombination can also be reduced by using CZTS layer as an HTM in PSCs.[25] Zuo *et al.* have employed CZTS nanoparticle as an HTM in lead based planar PSC and achieved a PCE of 13.41%.[26] They have also demonstrated an improved crystallinity of the perovskite film. In another work it has been exhibited that CZTS based PSC sustains more than 98% of its initial PCE for 3 days.[21] For ETM, TiO_2 is the most widely used materials both in planar and mesostructured PSC.[27] Currently the PCE of planar PSCs is lower than the mesostructured devices.[28] Apart from experimental works, a theoretical investigation is necessary to improve the performance of the planar PSC. Many researchers have used one dimensional solar cell capacitance simulator (SCAPS-1D) to simulate the PSC and other thin film solar cells.[29]

Recently, Kabir *et al.* have analyzed the $MAPbI_3$ based PSC with CZTS as the HTM, and optimized a few parameters such as absorber layer thickness and doping density of different layers to improve the PCE of the device.[30] In this paper, the defect density, doping concentration, and thickness of the absorber layer are varied to optimize the device performance. The effects of doping concentration and the electron affinity of the HTM and the ETM on the device performance have been investigated. The hole mobility of the HTM and the defect density at the ETM/absorber and absorber/HTM interfaces are also varied to improve the PCE of the device. This work will be very helpful to design a highly efficient lead based planar PSC with CZTS as the HTM.

2. Simulation Method and Device Model

Many researchers used the SCAPS-1D solar cell simulator to analyze the device performances such as quantum efficiency (QE), energy band diagram, *J*–*V* curve, fill factor (FF), power conversion efficiency (PCE), short circuit current density J_{sc} and open circuit voltage V_{oc}. Figure 1 shows the reference n–i–p planar PSC structure where the intrinsic absorber layer ($MAPbI_3$) is placed between the p-type HTM (CZTS) and the n-type ETM (TiO_2). The back metal contact is gold (Au) and the fluorine doped tin oxide (FTO) is a transparent conducting oxide. The values of shunt and series resistances of the reference PSC are 920.8 Ω·cm^2 and 9.8 Ω·cm^2, respectively.[25] For simulation, two nano-scale ($\sim$ 10 nm) hypothetical interface layers (IL1 and IL2) are added between the absorber and the ETM/HTM to consider the charge carrier recombination.[31]

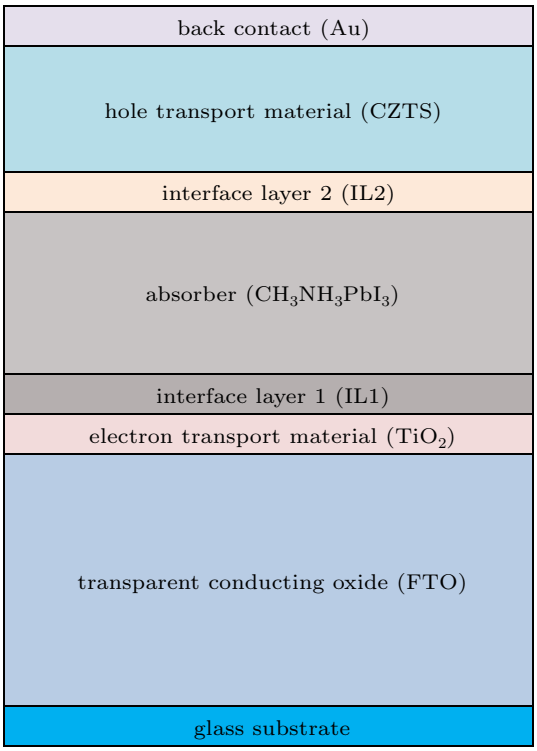


Fig. 1. Structure of an n–i–p planar PSC.

Table 1 shows the various material parameters of different layers considered in the simulation. The effective density states of valance band and conduction band are considered to be 1.8×10^{19} cm^{-3} and 2.2×10^{18} cm^{-3}, respectively.[32] At the back contact, the surface recombination velocities are considered to be 1×10^5 cm/s for electrons and 1×10^7 cm/s for holes.[32] At the front contact, the surface recombination velocities are assumed to be 1×10^7 cm/s for electrons and 1×10^5 cm/s for holes. The defect type is neutral with gaussian distribution and the characteristic energy is assumed to be 0.1 eV.[32] The value of capture cross section for both holes and electrons is taken as 1×10^{-15} cm^2. The work functions of front and back contacts are considered to be 4.41 eV and 5.10 eV, respectively.[32] The values of acceptor density, donor density and defect density of various layers are considered to validate the theoretical results with the experimental data.[25] All the simulations are performed under 1000 W/m^2 illumination, 1.5 G air mass and 300 K operating temperature.

Figure 2 shows the absorption coefficients (α) of different materials which are taken from Website.[38] These values are taken to avoid the empirical α calculated by the simulator. It is evident from Fig. 2 that $MAPbI_3$ has high α at wavelengths from 325 nm to 750 nm and hence absorbs most of the incident light at the visible spectrum. The peak value of α is at wavelength of 380 nm. Figure 2 also shows that CZTS has high

α at wavelengths from 325 nm to 1250 nm. The absorption coefficient of CZTS is nearly constant at wavelengths from 325 nm to 1000 nm and then falls sharply at wavelengths from 1000 nm to 1320 nm. It is evident from Fig. 2 that $MAPbI_3$ has higher α than CZTS up to 600 nm. Therefore CZTS contributes to the light absorption of the PSC from 600 nm to 1100 nm, which increases J_{sc} of the device. It is also evident from Fig. 2 that α of FTO decreases in the wavelength range from 325 nm to 560 nm since the extinction coefficient of FTO decreases up to wavelength 560 nm.[39]

Table 1. The material parameters of different layers considered in the simulation.

Parameters	CZTS (HTM)	IL2	$CH_3NH_3PbI_3$	IL1	TiO_2 (ETM)	FTO
Thickness/nm	200	10	265	10	35	350
Relative permittivity ε_r	7[36]	6.5	6.5[32]	6.5	100[32]	9
Electron affinity χ/eV	4.1[37]	3.91	3.91[9]	3.91	4[32]	4
Band gap E_g/eV	1.49[25]	1.56	1.56[33]	1.56	3.26[35]	3.5
Hole mobility μ_p/cm^2·V^{-1}·s^{-1}	20[37]	2	2[34]	2	0.006[32]	10
Electron mobility μ_n/cm^2·V^{-1}·s^{-1}	25[37]	3	3[34]	3	0.006[32]	20
Acceptor density N_A/cm^{-3}	1.7×10^{18}	–	–	–	–	–
Donor density N_D/cm^{-3}	–	5.6×10^{15}	5.6×10^{15}	5.6×10^{15}	4.4×10^{17}	9.1×10^{17}
Defect density N_t/cm^{-3}	5.1×10^{15}	9.1×10^{21}	1.4×10^{15}	8.4×10^{20}	10^{14}	1.78×10^{18}

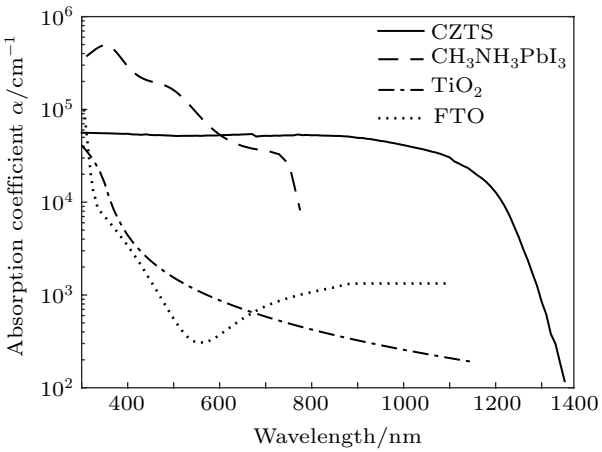


Fig. 2. Absorption coefficients of different materials.

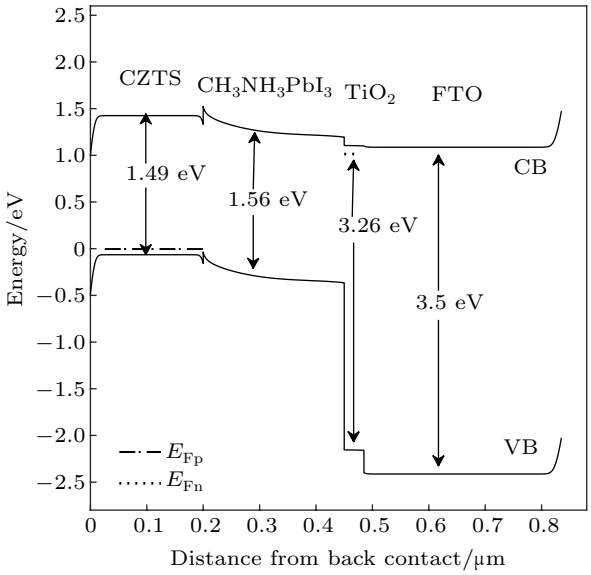


Fig. 3. Simulated energy band diagram of the device.

3. Results and discussion

3.1. Model validation

Figure 3 shows the energy band diagram of the reference PSC at equilibrium. It is evident from Fig. 3 that both the CZTS and $MAPbI_3$ act as absorber layers due to their apposite band gaps. It is also evident from Fig. 3 that the band offsets are suitable for the movement of charge carriers to the metal contact escaping recombination. Considering the parameters mentioned in Table 1, the device performance is obtained as V_{oc} of 1.06 V, J_{sc} of 20.49 mA·cm^{-2}, FF of 58.73% and PCE of 12.76%. It has been found that the simulated results are very close to the experimental data of CZTS based PSC.[25]

3.2. Effect of the defect density of the absorber on the PSC performance

The defect density of the absorber layer has a significant impact on the device performance. Absorber with larger grain size has lower defect density, longer diffusion length, and higher charge carrier mobility.[40] Figure 4 shows the effect of defect density on the device performance. The other

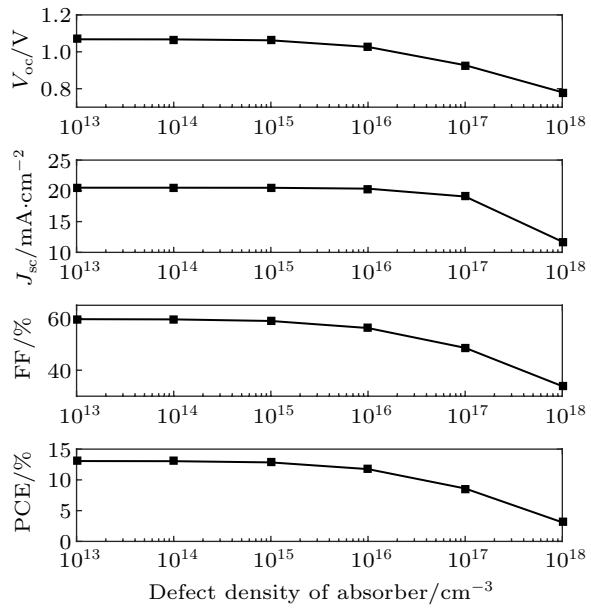


Fig. 4. Effect of defect density of absorber layer on the device performance.

device parameters are the same as those listed in Table 1. It is evident from Fig. 4 that V_{oc}, FF, J_{sc} and PCE do not change significantly up to defect density 10^{15} cm^{-3} and then decreases gradually. Low absorber defect density leads to longer diffusion length, which reduces the carrier loss due to recombination and hence the performance of the device improves. On the contrary, higher defect density causes shorter diffusion length and hence charge carrier recombination increases.[40,41] As a result, the device performance degrades significantly. Table 2 shows the relationship between the defect density and the diffusion length of the absorber layer. It is evident from Table 2 that the diffusion length of the charge carrier increases with the decrease in the defect density of the absorber layer. However, the electron diffusion length does not increase significantly by reducing defect density below 10^{14} cm^{-3}. The results will be useful for assessing perovskite film quality of lead based PSC.

Table 2. Variations of the charge carrier diffusion length with the defect density of absorber layer.

Defect density N_t/cm^{-3}	3.1×10^{17}	8.0×10^{16}	8.0×10^{15}	1.5×10^{15}	3.0×10^{14}	2.0×10^{14}	10^{14}
Diffusion length l_n/μm	0.05	0.1	0.3	0.7	1.6	2	2.8

3.3. Effect of the thickness of the absorber layer

The thickness of the absorber layer affects the device performance. Optimum absorber thickness ensures an efficient charge collection by balancing both absorption and recombination altogether in the device.[42] Figure 5 shows the device performance for various thicknesses of the absorber layer. The other device parameters are the same as those listed in Table 1. As the thickness of the absorber layer increases, V_{oc} increases up to 380 nm, and then decreases marginally. The generation rate of the charge carrier increases due to higher absorption of light. For thinner absorber, when the generation rate is higher than the recombination rate, the V_{oc} increases. Again for thicker absorber, when the recombination rate is higher than the generation rate, the V_{oc} decreases. Figure 5 shows that J_{sc} also increases with the absorber layer thickness up to 350 nm and then decreases. More excess carrier generates with the increase in thickness due to enhanced light absorption, and hence J_{sc} increases. The J_{sc} decreases when the absorber thickness greater than the charge carrier diffusion length due to enhanced recombination. Figure 5 also shows that the FF decreases continuously with the absorber thickness. It is evident from Fig. 5 that the PCE is maximal at $\sim$ 220 nm thickness. As the absorber thickness increases, more photon absorbs and hence, the PCE increases due to enhanced charge carrier generation rate. However for thicker absorber, the carrier transport is limited by the enhanced recombination which reduces the overall PCE. This happens when the thickness of the absorber layer is beyond the optimal value.[42,43]

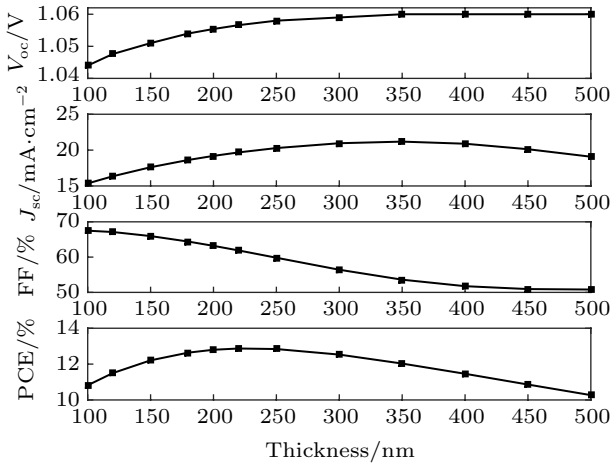


Fig. 5. Effect of the thickness of absorber layer on the device performance.

3.4. Effect of electron affinities of ETM and HTM

The band offset of the PSC structure plays an important role in determining charge carrier recombination at the interfaces.[44] It also quantifies the V_{oc} of the PSC. The band offsets can be tailored by changing the electron affinities of ETM and HTM. Figure 6 shows the effect of varying the electron affinity of the ETM on the device performance. The other device parameters are the same as those listed in Table 1. It is evident from Fig. 6 that V_{oc}, J_{sc}, FF, and PCE increase with the electron affinity of the ETM and then decrease gradually. The PCE decreases as the electron affinity decreases below 3.80 eV. The PCE also decreases as the electron affinity increases beyond 3.90 eV. The PCE is optimized at 3.85 eV electron affinity of the ETM.

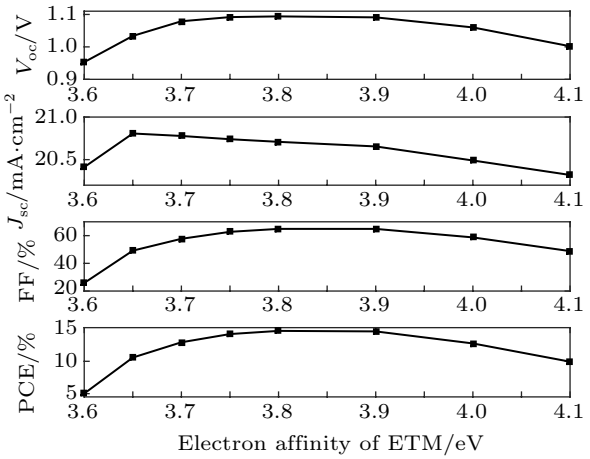


Fig. 6. Effect of electron affinity of ETM on the device performance.

Figure 7 shows the device performance by varying electron affinity of the HTM. The other device parameters are the

same as those in Table 1. It is noticeable from Fig. 7 that the V_{oc} decreases as the electron affinity decreases below 4 eV. The V_{oc} also decreases as the electron affinity of the HTM increases beyond 4.10 eV. However, J_{sc} decreases significantly as electron affinity increases beyond 3.90 eV. The device performance is optimized at 3.90 eV electron affinity of the HTM. Considering the optimized electron affinities for both the HTM and the ETM, the device performance is found as V_{oc} of 1.05 V, J_{sc} of 24.11 mA·cm^{-2}, FF of 61.28% and PCE of 15.57%.

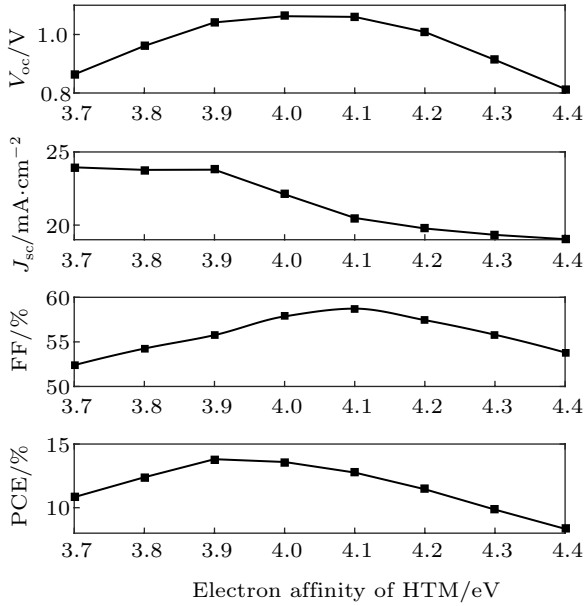


Fig. 7. Effect of electron affinity of the HTM on the device performance.

3.5. Effect of the defect density at the interface

The interface quality at the heterojunction affects the device performance. Specially, interface defect density at the absorber/ETM and absorber/HTM has a significant effect on the device performance.[31,32] Figure 8 shows the *J*–*V* characteristics of the PSC by varying defect density at the interface layer IL2. The other device parameters are the same as those in Table 1. It is evident from Fig. 8 that the defect density at IL2 does not affect the device performance significantly. Similar results have been demonstrated by another work.[32] Figure 9 shows the *J*–*V* characteristics of the PSC by varying defect density at the interface layer IL1. The other device parameters are the same as those in Table 1. It is noticeable from Fig. 9 that the *J*–*V* curve shifts downwards with the increase in defect density at IL1. As the defect density increases, more carriers are trapped at the interface and are not available for conduction. As a result, the device performance deteriorates.[32] The interface layer IL1 is closer to FTO than IL2 and hence, most of the charge carriers are generated near IL1. The presence of higher excess carrier near IL1 causes significant carrier loss due to trapping. As a result, defects at IL1 have more effects on the device performance than that at IL2. The similar effects for planar PSC structure have been observed by other researchers.[32] Therefore, a high quality absorber/ETM interface is essential for highly efficient lead based PSCs.

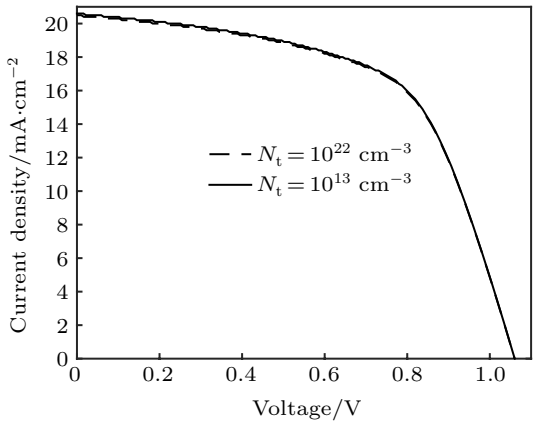


Fig. 8. *J*–*V* characteristics of PSC for various defect densities of IL2.

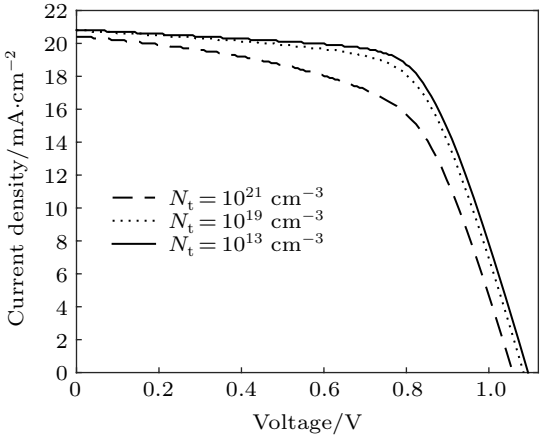


Fig. 9. *J*–*V* characteristics of PSC for various defect densities of IL1.

3.6. Effect of doping densities of absorber, ETM, and HTM

Doping plays a vital role to improve the performance of the halide based PSC. As doping density increases, charge carrier concentrations also increases. However, ionized impurity introduces scattering centers in the crystal structure which reduces the charge carrier mobility. Moreover, deep traps are generated due to high doping density.[45] Figure 10 shows the PCE of the PSC for various doping densities of the absorber, ETM, and HTM. Different ranges of doping density for three layers have been considered to show the significant effects. The other device parameters are the same as those in Table 1. Figure 10 manifests that the PCE of the PSC increases up to 2.0×10^{16} cm^{-3} doping density of the absorber layer and then decreases sharply. With the increase in doping density built in electric field enhances. As a result, the PCE of the device increases.[46] It is evident from Fig. 10 that the PCE increases for heavily doped ETM and HTM. The charge density increases with the increase in doping density, which increases the conductivity of the ETM/HTM and hence the PCE

of the device increases. It has been found that the PCE is optimum considering a doping density of 2.0×10^{18} cm^{-3} and 10^{19} cm^{-3} for the ETM and the HTM, respectively.

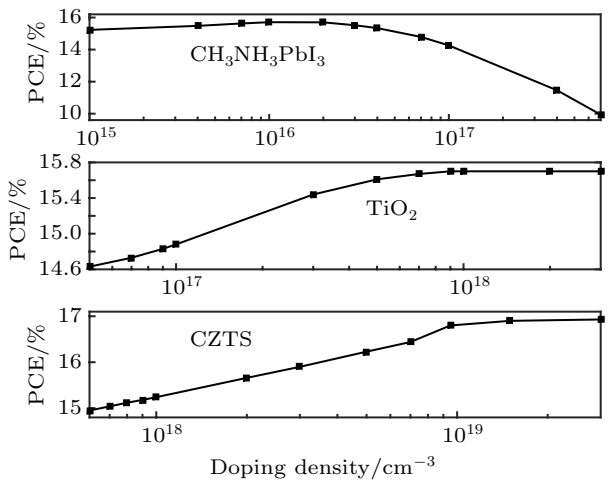


Fig. 10. The PCE of the PSC for various doping densities of the absorber, ETM, and HTM.

3.7. Determination of the optimized PSC structure

Table 3 shows the optimum parameters of the device. The comparison of the device performance considering the various optimum parameters and the reference structure parameters are shown in Table 4. The series resistance has a significant effect on the device performance. Considering all the optimum parameters and a series resistance R_s of 9.8 Ω·cm^2, the device performance is as V_{oc} of 1.15 V, J_{sc} of 26.29 mA·cm^{-2}, FF of 65.73%, and PCE of 19.83%. It has been reported that a lower R_s of ~ 5 Ω·cm^2 can be achieved in the planar lead based PSC.[43] For high performance thin film solar cells, R_s is less than 1 Ω·cm.[43] Considering all the optimum parameters and R_s of 5 Ω·cm^2, the final optimum device performance is as V_{oc} of 1.15 V, J_{sc} of 26.45 mA·cm^{-2}, FF of 74.61%, and PCE of 22.7%. The simulated optimum device performance is similar to the experimental data of mesostructured double-layered halide architecture with costly organic HTM.[47] Figure 11 shows the *J*–*V* characteristic curves of the PSC considering the optimum parameters and the reference structure parameters. The performance of the PSC can be improved further by fabricating a highly uniform perovskite layer with large grain size and long carrier diffusion length.[43]

Table 3. Optimum parameters of the device.

Parameters	HTM	IL2	Absorber	IL1	ETM
Thickness/ nm	–	–	220	–	–
Defect density N_t/cm^{-3}	–	10^{16}	10^{14}	10^{16}	–
Doping density/cm^{-3}	10^{19}	2×10^{16}	2×10^{16}	2×10^{16}	2×10^{18}
Electron affinity χ/eV	3.90	–	–	–	3.85

Table 4. Comparison of the performance between the reference structure parameters and the optimum parameters.

Parameters	Reference structure[25]	Optimum defect density and thickness of absorber	Optimum electron affinities of the HTM and ETM	Optimum defect density of IL1	Optimum doping density of absorber	Final optimization
J_{sc}/mA·cm^2	20.49	19.71	24.11	20.83	24.71	26.45
V_{oc}/V	1.06	1.06	1.05	1.09	1.05	1.15
FF/%	58.73	62.23	61.28	65.48	60.72	74.61
PCE/%	12.76	13.03	15.57	14.9	15.69	22.70

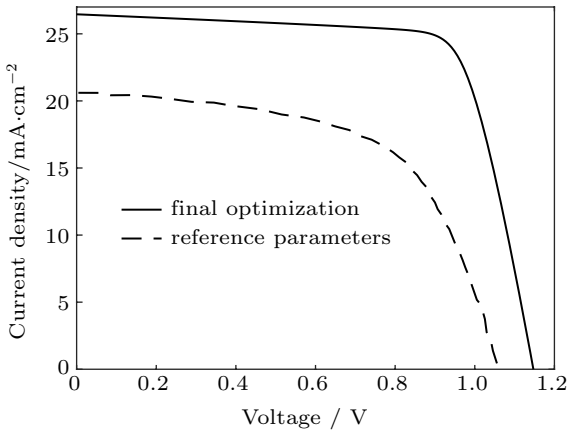


Fig. 11. *J*–*V* characteristics of the PSC. The dotted line and the solid line represent the simulated results considering the reference parameters and the optimum parameters, respectively.

As mentioned above, CZTS has also been used as an active layer in thin film solar cells. The best reported PCE of CZTS based thin film solar cell is 11%.[48] Various synthesis techniques have been used to improve the PCE of CZTS based photovoltaic devices. The complex synthesis process forms secondary phases which degrades the CZTS film quality and hence limits the solar cell efficiency.[49]

4. Conclusion

A lead based PSC with CZTS as inorganic HTM has been analyzed by SCAPS-1D device simulator. Consistent material parameters are taken from the literature. The relative permittivity, electron affinity, band gap, and charge carrier mobility of the absorber layer are the same as those in the reference structure. For the ETM and the HTM, the thickness, relative permittivity, band gap, and defect density are also the same as those in the reference structure. The simulated result illustrates that the performance of the reference PSC can be improved taking an optimum absorber layer defect density of $\sim 5 \times 10^{14}$ cm^{-3}. The optimum thickness of absorber layer ($\sim$ 220 nm) has been found, which increases the PCE. The doping in the absorber layer has also been optimized to increase the PCE from 12.76% to 15.69%. It has been observed that a doping density beyond 2×10^{16} cm^{-3} in the absorber

layer reduces the PCE of the device due to enhanced recombination rate. Electron affinities of 3.9 eV and 3.85 eV for the HTM and the ETM, respectively are found to increase the PCE of the reference PSC from 12.76% to 15.57%. It has also been found that the defect density at the absorber/HTM interface has negligible effect on the device performance. The defect density at the absorber/ETM interface has significant effect on the device performance as most of the carrier generated near this interface. The overall PCE of the reference PSC increases from 12.76% to 22.7% by considering a series resistance of 5 $\Omega{\cdot}\mathrm{cm}^2$, and the optimum parameters of absorber, ETM and HTM layers simultaneously. The PCE of the optimized PSC has been increased significantly compared to the reference structure. Hence, the optimized PSC structure with CZTS as the HTM is highly efficient.

References

[1] Park N G, Gratzel M, Miyasaka T, Zhu K and Emery K 2016 *Nat. Energy* **1** 16152

[2] Hawash Z, Ono L K and Qi Y 2018 *Adv. Mater. Interfaces* **5** 1700623

[3] Kim H S, Lee C R, Im J H, Lee K B, Moehl T, Marchioro A, Moon S J, Humphry-Baker R, Yum J H, Moser J E and Grätzel M 2012 *Sci. Rep.* **2** 591

[4] Liu D and Kelly T L 2014 *Nat. Photon.* **8** 133

[5] Jiang M, Niu Q, Tang X, Zhang H, Xu H, Huang W, Yao J, Yan B and Xia R 2019 *Polymers* **11** 147

[6] Kojima A, Teshima K, Shirai Y and Miyasaka T 2009 *J. Am. Chem. Soc.* **131** 6050

[7] Fakharuddin A, De Rossi F, Watson T M, Schmidt-Mende L and Jose R 2016 *APL Mater.* **4** 091505

[8] Werner J, Niesen B and Ballif C 2018 *Adv. Mater. Interfaces* **5** 1700731

[9] Noh J H, Im S H, Heo J H, Mandal T N and Seok S I 2013 *Nano Lett.* **13** 1764

[10] Baltakesmez A, Biber M and Tüzemena S 2018 *J. Radiat. Res. App. Scis* **11** 124

[11] Kim Y, Jung E H, Kim G, Kim D, Kim B J and Seo J 2018 *J. Adv. Energy Mater.* **8** 1801668

[12] Nia N Y, Matteocci F, Cina L and Carlo A D 2017 *ChemSusChem.* **10** 3854

[13] Wang Y, Hu Y, Han D, Yuan Q, Caoc T, Chen N, Zhou D, Cong H and Feng L 2019 *Org. Electron.* **70** 63

[14] Jena A K, Numata Y, Ikegami M and Miyasaka T 2018 *J. Mater. Chem. A* **6** 2219

[15] Ava T, Al-Mamun A, Marsillac S and Namkoong G 2019 *Appl. Sci.* **9** 188

[16] Hu L, Li M, Yang K, Xiong Z, Yang B, Wang M, Tang X, Zang Z, Liu X, Li B, Xiao Z, Lu S, Gong H, Ouyang J and Sun K 2018 *J. Mater. Chem. A* **6** 16583

[17] Heo J H, Han H J, Lee M, Song M, Kim D H and Im S H 2015 *Energy Environ. Sci.* **8** 2922

[18] Zhou P, Bu T, Shi S, Li L, Zhang Y, Ku Z, Peng Y, Zhong J, Cheng Y B and Huang F 2018 *J. Mater. Chem. C* **6** 5733

[19] Ye S, Sun W, Li Y, Yan W, Peng H, Bian Z, Lui Z and Huang C 2015 *Nano Lett.* **15** 3723

[20] Zuo C and Ding L 2015 *Small* **11** 5528

[21] Patel S B, Patel A H and Gohel J V 2018 *Cryst. Eng. Comm.* **20** 7677

[22] Li X, Yang J, Jiang Q, Chu W, Zhang D, Zhou Z and Xin J 2017 *ACS Appl. Mater. Interfaces* **9** 41354

[23] Xu L, Deng L L, Cao J, Wang X, Chen W Y and Jiang Z 2017 *Nanoscale Res. Lett.* **12** 159

[24] Yang S, Fu W, Zhang Z, Chen H and Li C Z 2017 *J. Mater. Chem. A* **5** 11462

[25] Wu Q, Xue C, Li Y, Zhou P, Liu W, Zhu J, Dai S, Zhu C and Yang S 2015 *ACS Appl. Mater. Interfaces* **7** 28466

[26] Zuo Y, Chen L, Jiang W, Liu B, Zeng C, Li M and Shi X 2018 *Mater. Tehno.* **52** 483

[27] Mahmood K, Sarwar S and Mehran M 2017 *RSC Adv.* **7** 17044

[28] Wang R, Mujahid M, Duan Y, Wang Z K, Xue J and Yang Y 2019 *Adv. Funct. Mater.* **1808843**

[29] Burgelman M, Decock K, Khelifi S and Abass A 2013 *Thin Solid Films* **535** 296

[30] Kabir I, Sadik F and Mahmood S A 2018 10*th International Conference on Electrical and Computer Engineering*, Dhaka, Bangladesh 20–22 December 2018, p. 145

[31] Chouhan A S, Jasti N P and Avasthi S 2018 *Mater. Lett.* **221** 150

[32] Tan K, Lin P, Wang G, Liu Y, Xu Z and Lin Y 2016 *Solid State Electron.* **126** 75

[33] Li H, Yang Y, Feng X, Shen K, Li H, Li J, Jiang Z and Song F 2016 *Nanomater Nanotechnol.* **6** 24

[34] Herz L M 2017 *ACS Energy Lett.* **2** 1539

[35] Chihi A, Boujmil M F and Bessais B 2017 *J. Electron. Mater.* **46** 5270

[36] Shin B, Gunawan O, Zhu Y, Bojarczuk N A, Chey S J and Guha S 2013 *Prog. Photovolt: Res. Appl.* **21** 72

[37] Wanda M D, Ouédraogo S, Tchoffo F, Zougmoré F and Ndjaka J M B 2016 *Int. J. Photoenergy* **1**

[38] https://www.pvlighthouse.com.au/refractive-index-library

[39] Sap J A, Isabella O, Jager K and Zeman M 2011 *Thin Solid Films* **520** 1096

[40] Ng A, Ren Z, Shen Q, Cheung S H, Gokkaya H C, So S K, Djurisic A B, Wan Y, Wu X and Surya C 2016 *ACS Appl. Mater. Interfaces* **8** 32805

[41] Zhou Y and Long G 2017 *J. Phys. Chem. C* **121** 1455

[42] Baloch A A, Hossain M I, Tabet N and Alharbi F H 2018 *J. Phys. Chem. Lett.* **9** 426

[43] Tavakoli M M, Gu L, Gao Y, Reckmeier C, He J, Rogach A L, Yao Y and Fan Z 2015 *Sci. Rep.* **5** 14083

[44] Lim K G, Ahn S, Kim Y H, Qi Y and Lee T W 2016 *Energy Environ. Sci.* **9** 932

[45] Thakur U, Kisslinger R and Shankar K 1996 *Nano Mater.* **7** 95

[46] Jiang C S, Yang M, Zhou Y, To B, Nanayakkara S U, Luther J M, Zhou W, Berry J J, Van De Lagemaat J, Padture N P, Zhu K and Al-Jassim M M 2015 *Nat. Commun.* **6** 8397

[47] Jung E H, Jeon N J, Park E Y, Moon C S, Shin T J, Yang T Y, Noh J H and Seo J 2019 *Nature* **567** 511

[48] Ravindiran M and Praveenkumar C 2018 *Renew. Sustain. Energy Rev.* **94** 317

[49] Zhang X, Fu E, Wang Y and Zhang C 2019 *Nanomaterials* **9** 336